
Supplementary Information

In situ approach of cementite nanoparticles encapsulated with nitrogen-doped graphitic shells as anode nanomaterials for Li-ion and Na-ion batteries

Na Na Li[§], *Zhao Min Sheng*[§*], *Hao Liang Tian, Cheng Kang Chang, Run Ping Jia and Sheng Han**

School of Materials Science and Engineering, Shanghai institute of technology,

Shanghai 201418, China

Materials characterization: All samples were characterized and analyzed by X-ray diffractometer (XRD; Bruker D8 Advance, Bruker AXS, Germany), high-resolution transmission electron microscopy (HRTEM; JEM-2100F, JEOL, Japan) and X-ray photoelectron spectroscopy (XPS).

Electrochemical measurements: The electrochemical behaviors were evaluated from performance of CR2016-type coin cells that were assembled in an Ar filled glove box. The working electrode was fabricated by a slurry coating procedure. First, the slurry was obtained by mixing active materials (Fe_3C@NGS), carbon black (super-p) and carboxyl methylated cellulose, at mass ratio 7:2:1 in distilled water. Then the slurry was coated on the copper foil and dried at 110 °C under vacuum for 3 hours. Pure lithium foil (for LIBs)/ sodium foil (for NIBs) was used as the counter electrode, and porous polypropylene (for LIBs)/ glass fiber (for NIBs) film as a separator. The electrolyte was composed of a solution of 1 M $LiPF_6$ in ethylene carbonate (EC), diethyl carbonate (DEC) and dimethyl carbonate (DMC) (1/1/1 in vol. %) for LIBs, (1M $NaClO_4$ dissolved in the solution with 1:1:1 EC, DMC and EMC by vol. % as the electrolyte for NIBs). After assembly, the cyclic voltammetry (CV) profiles and the galvanostatic charge-discharge measurements of the cells were carried out between 0.005 and 3V (*vs*. Li^+/Li, for LIBs) or between 0.005 and 2.5V (*vs*. Na^+/Na, for NIBs) on a CHI 760E electrochemical workstation and a battery test system (LAND CT-2001A tester), respectively. Electrochemical impedance spectrum (EIS) was measured on the electrochemical workstation (Autolab Pgstat302n) over a frequency range of 100 KHz to 0.05 Hz.

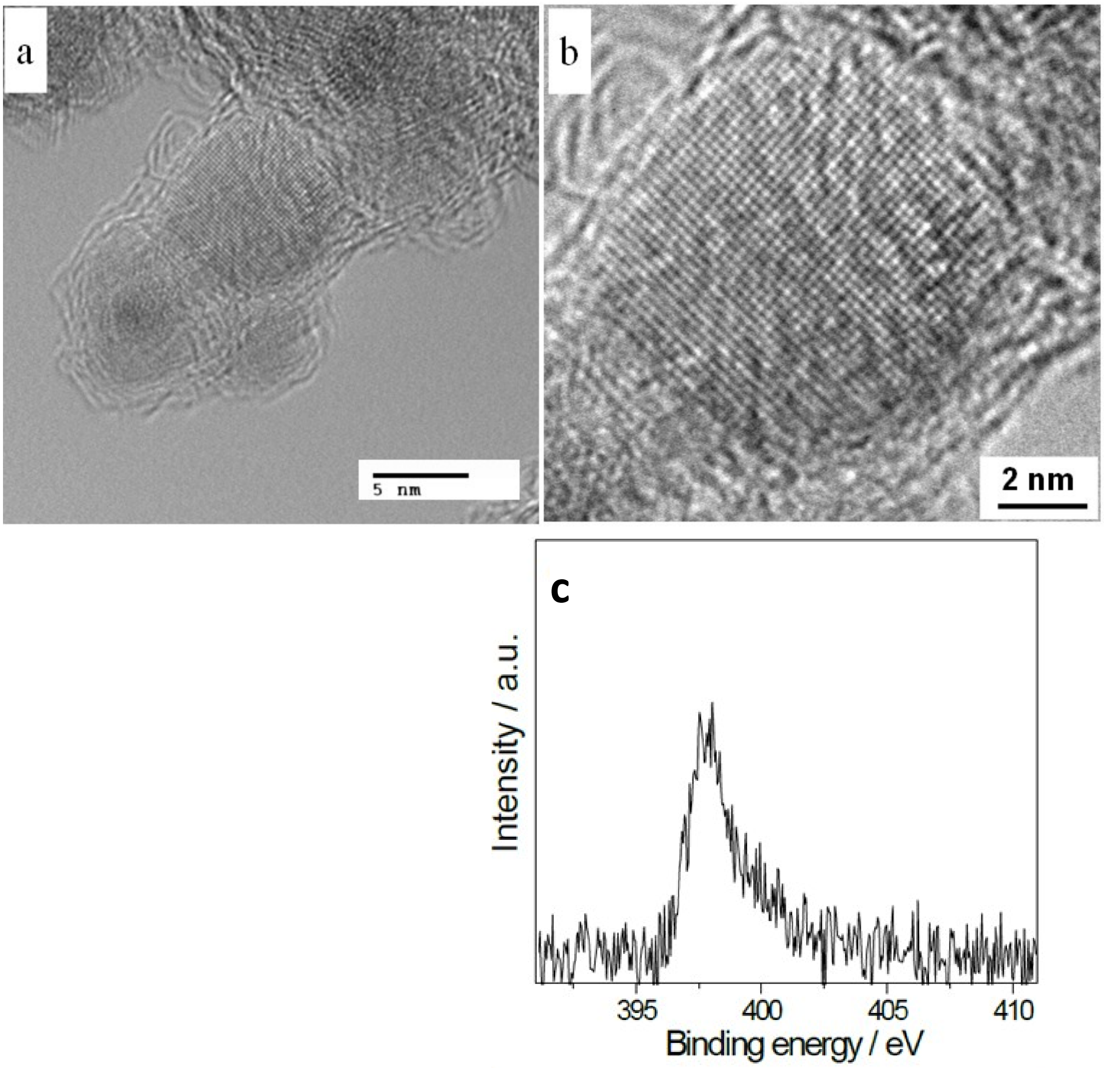

Fig. S1. (a) and (b) HRTEM images of nanoparticles (Fe_3C@NGS900) prepared at 900 ºC, and (c) XPS N1s spectrum of Fe_3C@NGS900.

The doping structure of graphitic shells has been measured by XPS. According to Fig. S2, the N 1s spectrum of Fe_3C@NGS900 locate at ~398 eV corresponding to pyridinic nitrogen and ~2 wt. % N atoms are doped on the surface of these nanoparticles. Such defects of the graphitic shells might offer channel for fast distribution of electrolyte and ions.

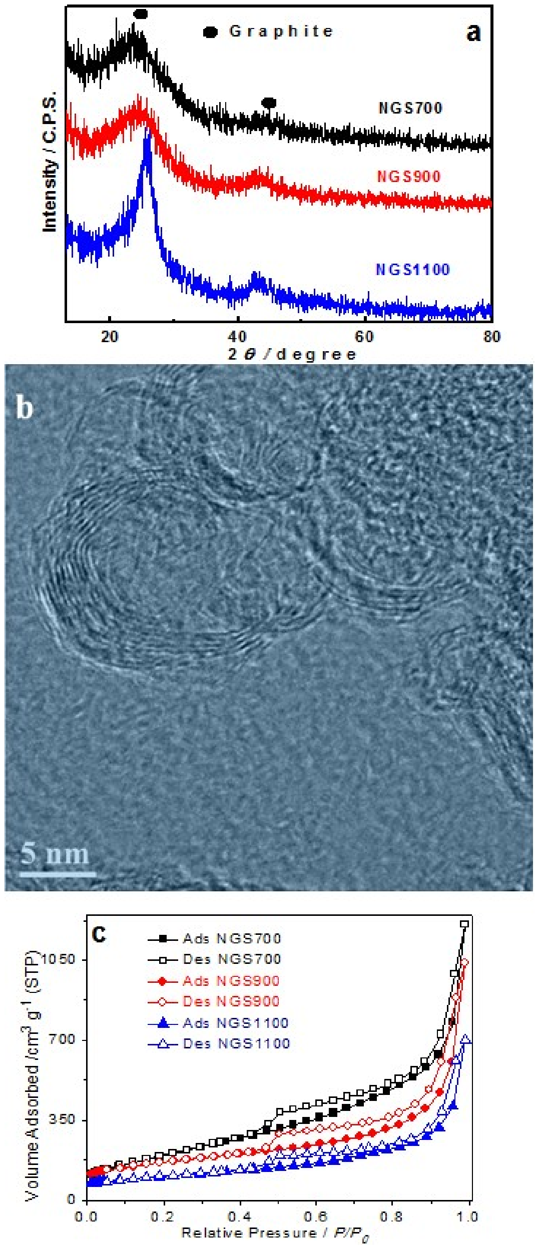

Fig. S2. XRD patterns (a), HRTEM image (b) and N_2 adsorption/desorption isotherms (c) of pure N-doped graphitic shells (NGS).

Ferrous cores have been removed to form pure N-doped graphitic shells (NGS) by acid-treatment (Fig. S2). The details of the experiment can be found in our previous work. In Fig. S2a, only diffraction peaks of graphite are shown, indicating the ferrous cores have been eliminated and carbonaceous nanocages have been prepared with inner hollow structure (Fig. S2b). The specific surface area (S_{BET}) and mesopore volume of these samples decrease with pyrolysis temperature increasing (700: 700 m^2 g^{-1} and 1.0 cm^3 g^{-1}; NGS900: 630 m^2 g^{-1} and 0.87 cm^3 g^{-1}; NGS1100: 445 m^2 g^{-1} and 0.52 cm^3 g^{-1}), according to isotherms shown in Fig. S2c.

$C_{Fe3C}= (C_{Fe3C@NGS}-C_{NGS}*(W_{NGS}))/W_{Fe3C}$ (equation S1)

Where C_{Fe3C}, $C_{Fe3C@NGS}$ and C_{NGS} are specific capacity of Fe_3C, Fe_3C@NGS900 and NGS900, respectively; W_{NGS} and W_{Fe3C} are weight percents of Fe_3C and NGS900, respectively.

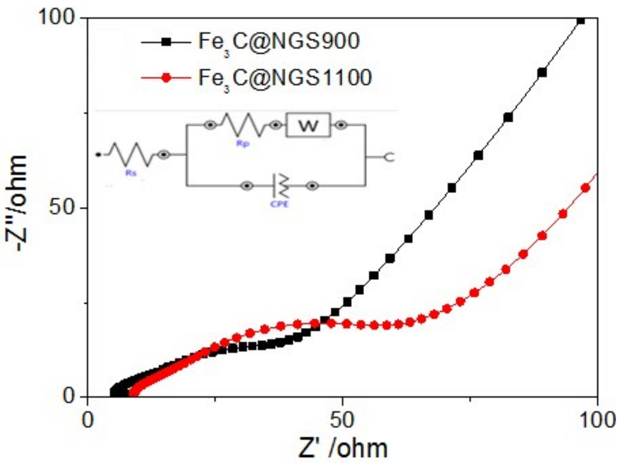

Fig. S3. EIS curves of the Fe_3C@NGS900 and Fe_3C@NGS1100 electrodes (the inset shows the common equivalent circuit).

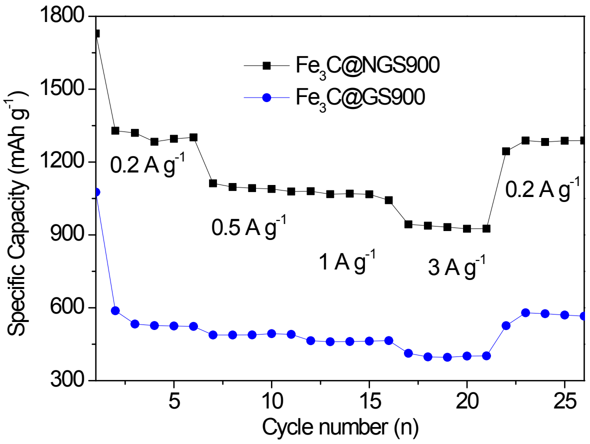

Fig. S4. charge-discharge cycling performance of Fe$_3$C@NGS900 and Fe$_3$C@GS900 core-shell nanoparticles at different current densities from 0.2 to 3 A g-1 at room temperature.

As shown in Fig. S4, the rate capabilities of Fe$_3$C@NGS900 and Fe$_3$C@GS900 anodes have been investigated at current densities of 0.2, 0.5, 1 and 3 A g^{-1} for every 5 cycles. At the corresponding rates, the reversible capacity are 1300, 1101, 1062 and 939 mA h g^{-1} for Fe$_3$C@NGS900; 575, 492, 458 and 402 mA h g^{-1} for Fe$_3$C@GS900, indicating N-doping of core-shell nanoparticles might enhance their electrochemical capability owing to lots flow channels prepared in Fe$_3$C@NGS900.